

# Deformation mechanisms of open-pit high-steep slopes controlled by a fault: An integrated remote sensing, field investigation and numerical simulation study

Anmin Jiang<sup>1</sup>, Daobing Zhang<sup>2</sup>, Feifei Wang<sup>3</sup>, Yanchen Dong<sup>4</sup>, Huadong Yin<sup>5</sup>, Huzhi Wang<sup>6</sup>, Sheng Zhang<sup>7</sup>, Zhicheng Duan<sup>8</sup>, Shaoxiang Xie<sup>9</sup>

<sup>1, 2, 5, 9</sup>School of Resource Environment and Safety Engineering, Hunan University of Science and Technology, Xiangtan Hunan, 411201, China

<sup>1, 4</sup>Department of Management Engineering, Hunan Urban Construction College, Xiangtan Hunan, 411101, China

<sup>3</sup>School of Civil Engineering, Hunan City University, Yiyang Hunan, 413000, China

<sup>6, 7</sup>The First Engineering Co. Ltd. of China Railway Wuju Group, Changsha, 410117, China

<sup>8</sup>Zhejiang University of Technology Engineering Design Group Co., Ltd, Hangzhou, 310014, China

<sup>3</sup>Corresponding author

**E-mail:** <sup>1</sup>jianganmin123@126.com, <sup>2</sup>dbzhang@hnust.edu.cn, <sup>3</sup>1942016362@qq.com,

<sup>4</sup>2314061293@qq.com, <sup>5</sup>hdyin1019@163.com, <sup>6</sup>812228753@qq.com, <sup>7</sup>253425357@qq.com,

<sup>8</sup>654385074@qq.com, <sup>9</sup>2298568176@qq.com

Received 8 June 2025; accepted 2 February 2026; published online 19 February 2026  
DOI <https://doi.org/10.21595/jme.2026.25109>



Copyright © 2026 Anmin Jiang, et al. This is an open access article distributed under the Creative Commons Attribution License, which permits unrestricted use, distribution, and reproduction in any medium, provided the original work is properly cited.

**Abstract.** The engineering disasters caused by fault structural zones represent a persistent challenge in geotechnical engineering. This study employs an integrated approach, combining multi-temporal remote sensing, field investigation, and numerical simulation, to investigate the deformation mechanisms and stability of an open-pit slope controlled by the F15 fault. The results demonstrate that the collapse of the northern slope results from the combined effect of the internal F15 fault structure and external unloading due to underground mining. Remote sensing imagery reveals a four-stage failure process: initial rock deformation, local landslides, local surface subsidence, and final surface subsidence. Significantly, the F15 structural zone alters the deformation trend of the upper slope, channeling displacement towards the eastern valley, with a maximum simulated displacement of 5.4 cm. The safety factor of the slope, calculated using the strength reduction method, is 1.45, and the potential sliding surface is identified as the F15 structural zone. While the slope is currently stable, the limited safety redundancy and observed local landslides highlight the need for targeted monitoring and reinforcement of the fault zone. This study provides data-supported insights for the prevention and control of geological disasters in similar fault-controlled mining slopes.

**Keywords:** mining engineering, fault structure, characteristics of slope deformation and failure, slope safety factor, numerical simulation.

## 1. Introduction

Fault zones represent one of the most critical geological factors controlling the stability of rock slopes in open-pit mining. During the transition from surface to underground extraction, slopes are subjected to complex coupling effects, including mining-induced unloading, blasting vibrations, and weathering. When such perturbations interact with pre-existing fault structures, the potential for large-scale landslides and collapses increases significantly [1-3]. As emphasized in the state-of-the-art review by Jiang et al. [4], the spatial variability introduced by fault systems must be adequately accounted for in any meaningful slope reliability analysis [5-7].

Significant research efforts have been devoted to understanding mining-induced slope deformation. For instance, Jiang et al. [8] used 3D numerical simulations to reproduce the evolution of plastic zones during ore extraction, revealing the failure mechanism of a slope undergoing open-pit to underground transition. Wei et al. [9] applied the discrete element method

(PFC2D) to model fracture development in overlying strata, illustrating the progressive caving process above underground workings. Liu et al. [10] and Qi et al. [11] also employed field investigations and numerical models to analyze landslide mechanisms in mining-disturbed rock masses. While these studies provide valuable insights into the role of mining unloading in slope instability, they often treat the rock mass as a relatively continuous medium, without explicitly addressing the dominant control exerted by large-scale fault structures on deformation patterns and failure mechanisms.

In recent years, extensive research has been conducted on slope stability under rainfall conditions, further enriching the understanding of the failure mechanisms of rock slopes. For instance, systematic experimental studies have been carried out on the instability mechanism and critical intensity of rainfall of high-steep rock slopes under unsaturated conditions, revealing the controlling effect of matric suction changes on slope stability [12]. Building on this, the effect of slope angle on fractured rock masses under the combined influence of variable rainfall infiltration and excavation unloading has been further explored, elucidating that steeply inclined slopes are more prone to progressive failure under combined external forces [13]. Other studies have focused on the evolutionary characteristics of the fracture network in rock slopes under the combined influence of rainfall and excavation, revealing the stage-wise patterns of crack propagation and coalescence through hydro-mechanical coupling simulations [14]. Additionally, image recognition methods for the deformation area of open-pit rock slopes under variable rainfall have been developed, providing new technical means for monitoring surface deformation of slopes [15]. However, these studies primarily focus on “rainfall-slope” interaction systems and have not systematically revealed the deformation mechanisms of slopes controlled by the combined effect of major fault zones and underground mining activities – which constitutes the core scientific issue addressed in this study.

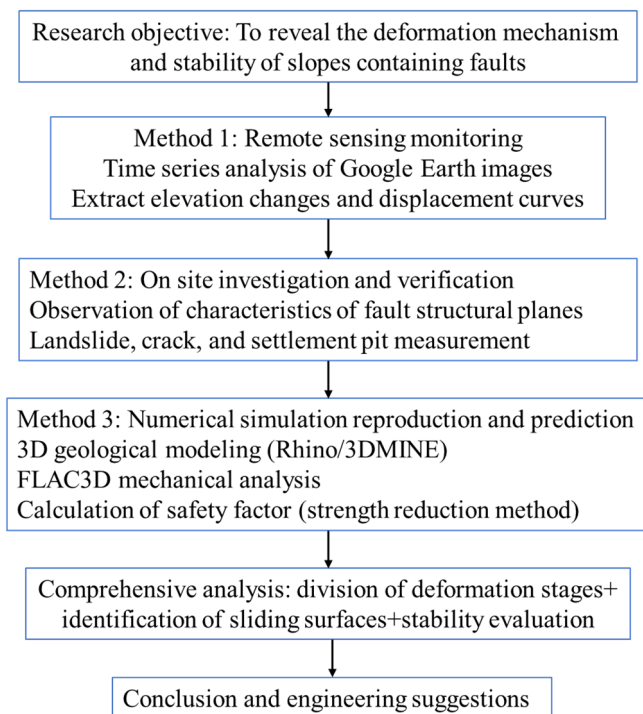


**Fig. 1.** Research methodology framework

The presence of a through-going fault zone such as F15 can severely disrupt slope integrity, alter failure trajectories, and serve as a preferential sliding surface. To address this research need,

the present study integrates multi-temporal remote sensing, field investigation, and 3D numerical simulation to systematically analyze the deformation mechanisms and stability of an open-pit slope controlled by the F15 fault. The specific objectives are: (1) to interpret the spatiotemporal evolution of slope deformation using satellite imagery; (2) to verify key deformation characteristics and structural controls through field surveys; (3) to reproduce the failure mechanism and identify the potential sliding surface via FLAC3D simulation; and (4) to evaluate the global stability of the slope using the strength reduction method. The integrated methodology adopted in this study is illustrated in Fig. 1, forming a closed loop from recognition and verification to mechanistic modeling and stability assessment.

The findings are expected to provide theoretical and practical guidance for the prevention and control of geological disasters in similar fault-controlled open-pit mining settings.

## 2. Geological and mining overview of the mining area

### 2.1. Stratigraphy and fault structure

The mining area is located in the southern section of the eastern wing of the syncline, with simple exposed strata, developed faults, joints, and fissures. No magmatic or metamorphic rocks have been found in the area, and the surrounding rock has undergone weak weathering. The Upper Cambrian Dengying Formation (Zbd) in the eastern, southern, northern, and central exposed strata of the mining area is divided into 8 layers, among which Zbd5, Zbd6, Zbd7, and Zbd8 layers are ore bearing layers.

The ore body is located in a graben type fault block structure in the southeast section of the transverse bridge inclined east wing, with F1 and F15 as boundaries. The fault block has a strike of about  $315^\circ$ , a length of about 15-20 km, and a width of about 150-600 m, and extends to the deep metamorphic rock series at a certain inclination angle. The development of fault fissures in the graben is the main ore conducting and hosting structure in the mining area.

The F15 is located in the northern part of the mining area, crossing the entire mining area from northwest to southeast, forming the northern boundary of the mining area's graben like structure. A "black fractured zone" is developed on the south side of the fault, and the mining area is rich in industrial ore bodies. It is 15-20 km long, 0.7-6.3 m wide, with a controlled extension depth of 240 m and a total fault displacement of 408m. It tends to be southwest or northeast with an inclination angle of  $56-89^\circ$ , and has a northwest trending fault. Before mineralization, it was a translational reverse fault, and after mineralization, it was a translational normal fault. The exposed location on the surface is shown in Fig. 2.



**Fig. 2.** F15 Exposed on the northern slope of the open pit.  
Photo by Wang Feifei, Sichuan, China, July 5, 2023

## 2.2. Rock mechanics parameters

To obtain the physical and mechanical parameters of the ore body and rock, indoor rock mechanics experiments were conducted to obtain the rock mechanics parameters. The RQD classification method, CSIR classification method for jointed rock masses, Q system classification method, GSI classification method, and geotechnical specification method were used to process the physical and mechanical test parameters of mining rocks [16-18]. The comprehensive rock mechanics parameters are shown in Table 1.

**Table 1.** Mechanical parameters of mineral rock mass

Rock material	Natural gravity $\gamma$ (kN/m <sup>3</sup> )	Elastic modulus $E$ (GPa)	Poisson's ratio $\mu$	Cohesion $C$ (MPa)	Internal friction angle $\varphi$ / (°)
Dolomite	28.0	8.09	0.22	1.50	45
Broken rock	29.0	1.04	0.29	0.20	15
Sandstone	26.9	3.35	0.27	0.55	30
Ore body	32.1	4.63	0.25	0.95	35
Backfill	21.0	2.63	0.23	0.5	23

## 3. Characteristics of deformation of slopes with fault structures

### 3.1. Development process of slope deformation and failure

To obtain the deformation and development process of the slope with fault structures, professional Google Earth software was used to obtain the process of the northern slope of the open-pit mining site gradually forming a landslide disaster from stability for a total of 10 years from 2012 to 2022. The typical remote sensing image is shown in Fig. 3-Fig. 6. Typical areas with significant changes were selected from the fault. On the Earth map, elevations were extracted for each year. And compared and analyzed the values over the years, and plotted the displacement change curve, as shown in Fig. 7.

According to satellite remote sensing images of deformation and failure of the northern slope of the open-pit mining site, local slope collapse has been occurring at the bottom of the northern pit since 2012. The main reason is that under the unloading effect of open-pit mining, the fault structure zone undergoes deformation and displacement, resulting in a weakened support effect at the bottom of the upper slope of the fault, leading to the deformation and failure of the slope. The remote sensing images from 2015 and 2012 are basically consistent, indicating that during this period, the mining disturbance caused by mining was relatively small, and there were no conditions for further development of slope collapse disasters.

In the remote sensing image of 2017, it can be clearly seen that there is a phenomenon of local step slope rock fragmentation and collapse in the upper part of the northern slope (white spot in the figure). The area where the original collapse occurred at the bottom has not further expanded. During this period, the impact of underground mining on the open-pit mining slope gradually developed towards the surface, and from 2012 to 2015, it had not yet developed to affect the surface slope. Around 2017, signs of underground mining affecting the slope began to appear.

From the satellite images in 2020, it can be seen that multiple collapses have occurred on the northern slope of the open-pit mining area. The local step slope fragmentation zone in the upper part of the slope has been connected to the bottom collapse zone, forming a collapse zone centered on F15. The continuous expansion of the goaf formed by underground ore body mining has affected the stability of the northern slope. The lower part of the slope has experienced unloading, resulting in a sliding and collapsing phenomenon of the broken body, that is, the occurrence of landslides and holes. Due to the development of the F15 in the northern slope area, under the unloading effect of the lower ore body mining, the slope will experience displacement deformation along the fault, further exacerbating the damage to the northern slope and causing landslides. Over time, the northern slope may develop into a large-scale landslide disaster.

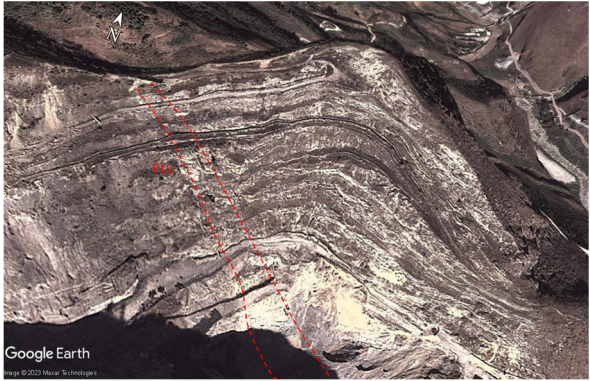


**Fig. 3.** Satellite image from December 2012



**Fig. 4.** Satellite image from December 2015

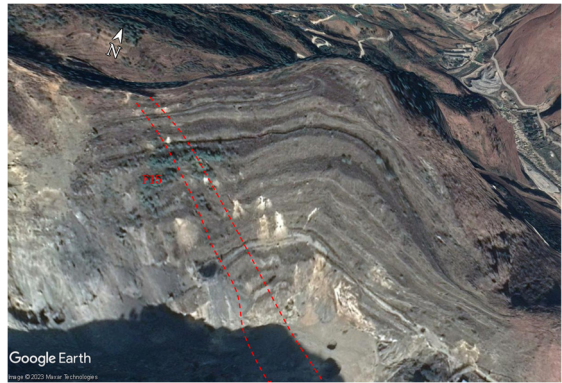


**Fig. 5.** Satellite image from December 2017

According to Fig. 7, the rock mass at the fault gradually developed and failed during the period of 2012-2017. After 2017, rapid displacement changes occurred, indicating significant displacement of the rock mass at the fault. The fault is rapidly breaking down. Significant damage has occurred on the northern slope.

### **3.2. Characteristics of damage to open-pit slopes**

To obtain the deformation and failure characteristics of the northern slope of the open-pit mining area, a field investigation and analysis method was used to obtain the typical failure characteristics of the northern slope of the open-pit mining area. As shown in Fig. 8, a landslide

collapse phenomenon occurred in the northern slope of the fault structure zone. The rocks in the fault structure zone are highly fragmented and weathered, which accelerates the deformation and damage of the exposed fault structure zone after rainwater erosion. Recent studies on the micro-scale deterioration of sandstone have shown that water-rock interactions, including mineral dissolution and micro-crack propagation driven by cyclic wetting-drying, can lead to significant strength reduction [19-20]. This micro-mechanism provides a plausible explanation for the macroscopic weakening of the F15 fault zone materials observed in the field. Due to the collapse and collapse of the goaf formed by underground mining, surface subsidence pits were formed at the bottom of the open-pit mining area, as shown in Fig. 3. The fault structure zone exposed on the slope has formed multiple cracks with a width of about 1m under the erosion of rainwater. The platform of the northern slope at the location of the fault tension joint experienced a 2.1 m subsidence and displacement, mainly due to the collapse of the underground goaf, which caused the large rock mass between the fault and the goaf to tilt and sink, resulting in platform subsidence and displacement, and the appearance of tensile cracks.



Fig. 6. Satellite image from December 2020

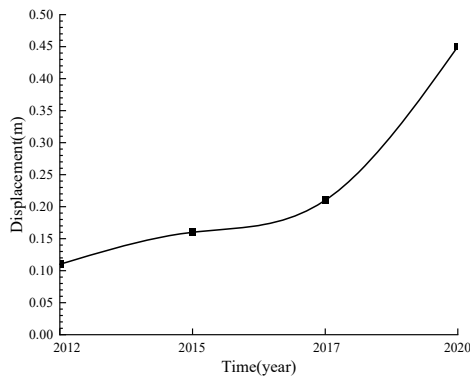


Fig. 7. Typical displacement variation curve at the fault

The mine adopts the bottomless pillar segmented collapse method to mine the underground ore body. After the ore body is mined, the overlying rock strata of the ore body are disturbed by mining, resulting in longitudinal and transverse cracks. Due to the presence of structural planes in the original rock and on-site measurements, it is known that there are structural planes with dip angles close to vertical and horizontal in both the overlying sandstone and dolomite bodies. Under the disturbance of mining and blasting, some roof rock masses collapsed and collapsed into the goaf, and the volume of the goaf gradually expanded towards the surface. After multiple overlying rock layers collapsed and fell to the surface, the pressure arch formed by continuous development in the early stage was destroyed, making it difficult for the overlying rock layers to self-stabilize.

Under the continuous disturbance of underground mining and heavy rainfall seepage, the overlying large rock mass gradually collapsed and collapsed, eventually leading to surface subsidence. There is an F15 trending towards the northeast on the western and northern slopes, with a distance of about 100 meters from the ore body. As the ore body is gradually mined, the formed goaf gradually expands, and the overlying rock strata collapse, affecting the stability of the fault and causing the large rock mass between the goaf and the fault to gradually tilt towards the goaf, resulting in tipping type damage. At present, according to on-site investigation, there have been significant tension joints at the fault location.



**Fig. 8.** Dangerous rock mass group on the hillside.  
Photo by Wang Feifei, Sichuan, China, July 5, 2023

Through remote sensing images and on-site investigation and analysis, it is found that the collapse disaster of the northern slope is the result of the combined action of internal fault structures and external underground ore body mining unloading. Under the disturbance of underground ore body mining, the northern slope is prone to landslide collapse along the fault structure zone and continuously expand the landslide area due to the cutting effect of the F15.

## 4. Analysis of numerical simulation models

### 4.1. Computation model

A numerical model that can accurately reflect the geological conditions of mining engineering is a prerequisite for simulating the landslide evolution of open-pit mining caused by underground ore body mining. Based on the current technical data of mining operations, multiple software (Rhino, 3DMINE, AUTOCAD) are used to jointly establish a three-dimensional model that includes the original terrain of the mine, underground ore bodies, and various surrounding rock bodies. By using Kubrix and Griddle plugins to mesh a three-dimensional model containing multiple rock types and geological structures, a FLAC3D mechanical analysis model that can run calculations in finite difference software was obtained.

The numerical simulation adopts the Mohr-Coulomb elastoplastic constitutive model, which effectively simulates the plastic yielding behavior of rock masses under shear and tensile stresses. While more advanced constitutive models, such as the non-orthogonal plastic damage model developed by Zhou et al. [21] for concrete, can capture complex material behaviors, the Mohr-Coulomb criterion remains a robust and widely validated model for simulating the shear failure of rock masses, especially when the failure is structurally controlled by pre-existing planes of weakness like the F15 fault. The model employs tetrahedral elements for meshing, with local mesh refinement applied in the F15 fault zone and goaf areas. The minimum element size is 5 m, and the maximum is 20 m, ensuring accurate stress-strain solutions in critical regions.

The boundary conditions are established based on Saint-Venant's principle and engineering

scale analysis: Lateral boundaries: Sliding hinge supports (restricting displacement in  $X$  and  $Y$  directions) simulate the lateral constraint of infinite rock mass on the study area; Bottom boundary: Fixed hinge supports (restricting displacement in  $X$ ,  $Y$ , and  $Z$  directions) represent the rigid support of deep intact bedrock; Ground surface: Free surface without constraints.

Mesh sensitivity analysis was conducted to verify the convergence of computational results. When the number of elements increased from 800,000 to 1,200,000, the maximum displacement variation was less than 2 %, indicating that the current mesh density ensures computational accuracy.

The numerical calculations utilize the rock mass mechanical parameters shown in Table 1, with the tensile strength of the rock mass considered as 10 % of the cohesion. The computational process includes three main steps: initial geostatic stress balance, sequential simulation of underground ore body mining, and slope safety factor calculation using the strength reduction method.

The establishment of an engineering scale model that conforms to specific engineering geological conditions is a prerequisite for conducting simulation calculations. Therefore, it is necessary to process the model boundaries before calculation. Scholars [22-23] have conducted studies on the influence of boundary conditions in numerical simulations, and the results show that when the length and width of the studied structure (ore body) are greater than 3-5 times, the influence of boundaries on the numerical simulation results can be ignored. The established 3D model measures 1152.43 m in length, 886.88 m in width, and 395.65-1065.10 m in height. The length of the ore body is 300-450 m, which meets the requirements of the boundary conditions. Restricting nodes in the  $X$  and  $Y$  directions on the boundary plane around the model, i.e. implementing sliding hinge supports. Restricting nodes in the  $X$ ,  $Y$ , and  $Z$  directions on the bottom plane of the model, i.e. achieving fixed hinge supports. The surface is a free surface without any restrictions [24-25]. The three-dimensional numerical simulation adopts the Mohr Coulomb constitutive model. The process of numerical simulation mainly includes stress balance analysis, calculation of underground ore body mining process, and calculation of slope safety factor by strength reduction method.

## 4.2. Analysis of slope deformation and displacement

Based on the previous remote sensing identification and on-site investigation results, this section further analyzes the deformation response and stability of slopes under fault control through numerical simulation methods. The deformation displacement of the slope during underground mining was calculated using three-dimensional numerical simulation. The typical displacement cloud map is shown in Fig. 9. The numerical simulation result is the cloud map of the results after the mining is completed in the future.

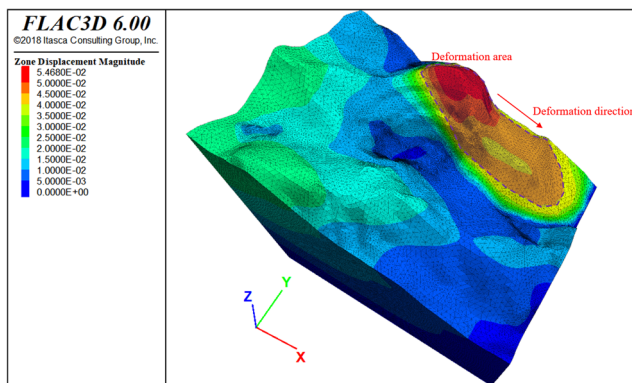


Fig. 9. Cloud map of slope deformation and displacement

According to the deformation displacement cloud map of the open-pit mining slope in Fig. 9, the focus of this study is on the relatively large deformation displacement at the top of the northern slope, which gradually decreases in the bottom direction, with a maximum displacement of 5.4 cm. The deformation displacement occurring below the F15 zone is relatively small. The main reason is the void formed after underground ore body mining, which provides spatial conditions for the rock mass below the fault structure zone to deform deeper, so the possibility of deformation and failure towards the east is relatively small. The deformation displacement of the rock mass above the potential sliding surface develops along the F15 structural zone towards the eastern valley, indicating that the F15 structural zone has changed the deformation and failure trend of the upper slope of the northern slope. With the mining of underground ore bodies, the impact on the upper open-pit mining area gradually increases. Finally, the underground mining of the ore body caused deformation of the northern slope. Landslides may occur on the northern slope, and the potential sliding arc surface is a fault fracture zone.

In this study, to investigate the impact of mining orebodies near faults on northern slopes, multiple horizontal mining levels were simulated. We extracted vertical surface displacement after the simulation and obtained maximum vertical displacement contour maps and data. The results are shown in Fig. 10.

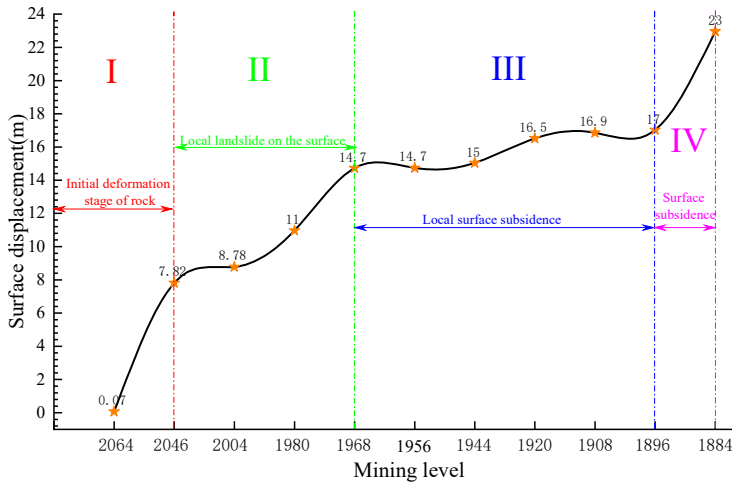


Fig. 10. Relationship between mining level and surface displacement

Fig. 10 indicates that after mining the 2004 level, the slope displacement reached 8.78 m, showing the mountain is in the landslide stage, consistent with the actual site. This confirms the numerical simulation results are reliable.

From Fig. 10, as mining levels deepen, displacement increases. During surface displacement development, three inflection points appear at the 2046, 1968, and 1896 levels, dividing the process into four stages. Currently, the mountain is in the second stage with local landslides. Severe landslides or collapses are expected when mining the 1968 level. Maximum displacement is 22.96 m in the final stage, and minimum displacement is 0.07 m in the initial stage.

Surface landslides and final collapses develop through four stages: initial deformation stage of rock, local landslide on the surface, local surface subsidence, surface subsidence. Deformation and cracking first appear, then landslides, and finally collapses.

Each stage has a different formation mechanism. Initially, after mining the 2064 level, the overlying rock partially collapses and fractures due to disturbance, causing gradual deformation of the overlying rock. During mining, fractures in the overlying repeatedly rock are disturbed and expand under water influence. The rock collapses, causing local surface settlement and landslides. After landslides form, continued collapse and water action create multiple subsidence holes. The

landslide worsens as the rock collapses in many areas. After extensive collapse of the overlying rock to the surface, it becomes unstable. Underground mining disturbance leads to surface subsidence.

### 4.3. Slope shear strain and safety factor

According to the Technical Code for Slope Engineering of Non-Coal Open Pit Mines GB51016-2014 [26], the allowable safety factor of the slope under normal conditions is 1.25-1.20. The safety factor is used to evaluate the stability of the northern slope of the open-pit mine after underground mining. The shear strain and safety factor are shown in Fig. 11.

According to the shear strain increment cloud map in Fig. 11, it can be seen that the deformation and failure of the upper rock mass of the northern slope mainly develop towards the east. The area with the largest increase in shear strain is the F15 zone, where the slope mainly exhibits a flat shear failure mode. This finding underscores that the presence of a dominant geological structure dictates the failure mechanism. Similar to the observations by Ma et al. [27] in underground structures, where structural components and interfaces controlled seismic failure patterns, the F15 fault in this study acts as the primary structural control governing the slope's failure mode. According to the on-site investigation results, it is known that a landslide disaster occurred along the F15 structure zone on the northern slope, which is consistent with the numerical simulation results, indicating the reliability of the numerical simulation results.

The safety factor of the open-pit mining slope calculated by the finite element strength reduction method is 1.45, and the potential sliding surface is the F15 structure zone, indicating that there has not been significant deformation and damage along the fault structure zone in the northern slope. The on-site investigation results show that there is a local collapse disaster in the fault structure zone inside the mining site, which is consistent with the numerical simulation results. The safety factor of the slope meets the requirements of the specifications, but the redundancy of the safety factor is small. With the continuous weathering, collapse, and disturbance and damage of the fault structure zone by underground mining, serious large-scale landslide disasters may occur in the later stage of the fault structure zone. Targeted measures can be taken by monitoring the deformation displacement and slope stress of open-pit mining slopes to prevent landslide disasters from posing safety hazards to mining production.

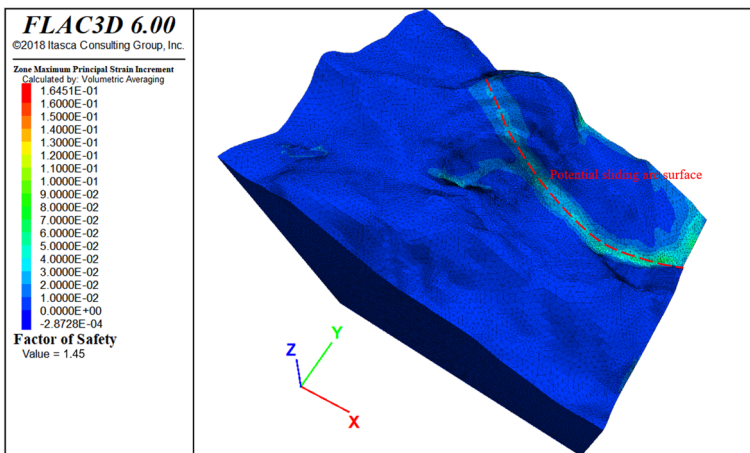


Fig. 11. Slope shear strain and safety factor

## 5. Discussion

The findings of this study regarding the controlling role of the F15 fault in slope deformation and failure gain deeper significance when compared with established theories and previous case

studies. The numerical simulation results clearly identify the F15 structural zone as the potential sliding surface, a phenomenon consistent with the Hoek-Brown failure criterion, which emphasizes the dominance of pre-existing, persistent geological structures in rock mass strength [16]. The shear strain increment concentrated along the F15 zone (Fig. 10) underscores its role as a plane of weakness, drastically reducing the overall integrity of the slope mass. This mechanism aligns with observations in other mining-related landslides, where fault zones act as preferential pathways for failure [3, 7].

Furthermore, the four-stage failure process (initial deformation → local landslide → local subsidence → surface subsidence) revealed through remote sensing and simulation is not merely a description of events but reflects a progressive failure mechanism. The initial deformation stage corresponds to the yield and fracture initiation within the rock mass above the goaf. The subsequent local landslides and subsidence signify the formation and coalescence of internal damage, a process exacerbated by the presence of the F15 fault, which provides a continuous boundary for the failure volume. This progressive failure pattern shares similarities with the “step-path” failure mechanism often observed in jointed rock masses, but here, the F15 fault serves as the dominant, large-scale “step” that governs the entire failure trajectory [17]. Compared to the study by Jiang et al. [8], which focused on the plastic zone evolution in a similar open-pit to underground transition, our research quantitatively highlights the paramount influence of a single, major fault structure in dictating the location and mode of the ultimate slope failure.

This study systematically reveals the controlling effect of the F15 fault on slope deformation and stability through a three in one research method of “remote sensing recognition on-site verification numerical simulation”. The three methods complement each other at the spatial scale, time series, and mechanism levels, jointly constructing a complete cognitive chain from phenomena to mechanisms. The study provides a comprehensive analysis of the impact of fault structures on the deformation, failure characteristics, and stability of open-pit high-steep slopes. Below is a detailed discussion of the key findings:

Fault structures are identified as crucial factors affecting the stability of open-pit slopes. The research emphasizes that the existence of fault structures within slopes can significantly influence slope stability by cutting the slope and reducing its integrity. This is supported by the case study of the open-pit mining site where the F15 fault structure zone plays a pivotal role in the deformation and failure of the northern slope. The study reveals that the fault structure zone not only weakens the mechanical properties of the slope but also alters the deformation and failure trend of the upper slope of the northern slope. This finding aligns with previous research that highlights the detrimental effects of fault structures on slope stability.

The research highlights the combined action of internal fault structures and external factors such as underground ore body mining unloading. It is found that the collapse disaster of the northern slope results from this coupling effect. Underground mining activities disturb the stress field around the slope, leading to deformation and displacement of the fault structure zone. This further weakens the support effect at the bottom of the upper slope of the fault, ultimately causing slope deformation and failure. This combined action mechanism provides a more comprehensive understanding of the factors contributing to slope instability in open-pit mining areas.

The study offers valuable insights into the development process of slope deformation and failure. Based on remote sensing images and field investigations, it is revealed that the northern slope of the open-pit mining site undergoes a four-stage development process of slope deformation and failure. This process begins with the initial deformation stage of rock and progresses through local landslide on the surface, local surface subsidence, and finally surface subsidence. The identification of these stages helps in understanding the temporal and spatial evolution of slope deformation and failure, which is crucial for early warning and prevention of slope disasters.

Numerical simulation plays a vital role in this study, providing detailed information on slope deformation, displacement, shear strain, and safety factor. The results indicate that the deformation displacement of the slope above the F15 zone is relatively large and develops towards the eastern valley along the F15 zone. This is consistent with the field investigation results,

confirming the reliability of the numerical simulation. The safety factor calculation shows that the open-pit slope has a safety factor of 1.45, with the potential sliding surface being the F15 structure zone. Although the safety factor meets the regulatory requirements, the small redundancy suggests that targeted measures should be taken to monitor and prevent slope disasters.

The findings of this study have practical implications for the prevention and control of geological disasters in similar mines. By understanding the impact of fault structures on slope stability and the deformation and failure process, mining companies can develop effective monitoring and early warning systems to ensure safe production. However, there are still some limitations in this study that need to be addressed in future research.

One limitation is the relatively small number of case studies, which may affect the generality of the conclusions. Future research could expand the study area to include more open-pit mining sites with different geological conditions and fault structures. Additionally, more advanced technologies and methods, such as remote sensing monitoring and real-time slope deformation monitoring systems, could be integrated to enhance the accuracy and reliability of the research results. Furthermore, the long-term stability analysis of slopes under the combined action of multiple factors, such as climate change and mining activities, could be explored in depth to provide more comprehensive guidance for slope stability control.

In conclusion, this study contributes to a deeper understanding of the impact of fault structures on the deformation and failure characteristics and stability of open-pit slopes. The findings provide valuable references for the prevention and control of geological disasters in open-pit mining areas. Future research should continue to explore this field to further improve the safety and stability of open-pit slopes.

## 6. Conclusions

This study integrated remote sensing, field investigation, and numerical simulation to investigate the deformation mechanisms and stability of an open-pit high-steep slope controlled by the F15 fault. The main conclusions, along with their specific engineering implications, are as follows:

1) The collapse disaster of the northern slope is the result of the combined action of the internal F15 fault structure and external unloading from underground ore body mining. Under mining disturbance, the slope is prone to landslides along the F15 zone, with the landslide area continuously expanding.

2) The F15 structural zone fundamentally alters the deformation trend of the northern slope, channeling displacement towards the eastern valley. The failure develops through four distinct stages: initial rock deformation, local landslides, local surface subsidence, and final surface subsidence.

3) The safety factor of the open-pit mining slope is 1.45, and the potential sliding surface is the F15 structure zone. Currently, the northern slope has not experienced significant deformation or damage along the fault structure zone. The on-site investigation results show that there is a local collapse disaster in the fault structure zone of the mining site, which is consistent with the numerical simulation results.

## Acknowledgements

This work was supported by the Natural Sciences Funding Project of Hunan Province (2024JJ6110, 2026JJ80763), Application Basic Research and Soft Science Research Plan of Yiyang City (2024YR02), Excellent Youth Project of the Education Department of Hunan Province (25B0685).

## Data availability

The datasets generated during and/or analyzed during the current study are available from the corresponding author on reasonable request.

## Author contributions

Jiang Anmin wrote the initial draft (including substantive translation). Zhang Daobing, Wang Feifei and Dong Yanchen carried out the software analysis. Yin Huadong, Wang Huzhi, Zhang Sheng, Duan Zhicheng and Xie Shaoxiang carried out the site investigation.

## Conflict of interest

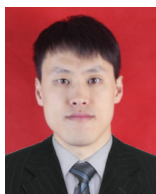
The authors declare that they have no conflict of interest.

## References

- [1] Wang Feifei et al., “Numerical simulation of progressive development process of surface subsidence caused by underground complex goaf,” *Mining and Metallurgical Engineering*, Vol. 40, No. 11, pp. 22–25, 2020.
- [2] Wang Feifei et al., “Study on the formation and development mechanisms of surface subsidence in Chaganaobao iron-zinc mine,” (in Chinese), *Rock and Soil Mechanics*, Vol. 41, No. 11, pp. 3757–3768, 2020, <https://doi.org/10.16285/j.rsm.2020.0128>
- [3] F. Wang, Q. Ren, X. Jiang, J. Niu, and B. Chen, “Engineering geology and mechanism of multiple landslides in a large open-pit mine: the case of the Copper Mine in Qinghai Province, China,” *Bulletin of Engineering Geology and the Environment*, Vol. 82, No. 4, p. 147, Mar. 2023, <https://doi.org/10.1007/s10064-023-03186-4>
- [4] S.-H. Jiang, J. Huang, D. V. Griffiths, and Z.-P. Deng, “Advances in reliability and risk analyses of slopes in spatially variable soils: A state-of-the-art review,” *Computers and Geotechnics*, Vol. 141, p. 104498, Jan. 2022, <https://doi.org/10.1016/j.compgeo.2021.104498>
- [5] F. Wang et al., “Strata movement law based on progressive caving of the hanging wall: a case of study in Chaganaobao Iron-Zinc Mine,” *Arabian Journal of Geosciences*, Vol. 13, No. 21, pp. 1155–1170, Oct. 2020, <https://doi.org/10.1007/s12517-020-06112-0>
- [6] F. Wang, Q. Ren, and B. Chen, “Numerical investigation on safe mining of residual pillar in goaf: A case study of Panlong Lead-zinc Mine,” *Geotechnical and Geological Engineering*, Vol. 38, No. 38, pp. 4269–4287, 2020.
- [7] G. Ma, X. Hu, Y. Yin, G. Luo, and Y. Pan, “Failure mechanisms and development of catastrophic rockslides triggered by precipitation and open-pit mining in Emei, Sichuan, China,” *Landslides*, Vol. 15, No. 7, pp. 1401–1414, May 2018, <https://doi.org/10.1007/s10346-018-0981-5>
- [8] A. Jiang, Y. Dong, and X. Jiang, “Numerical simulation of open pit slope collapse caused by transition from open pit to underground mining,” *Mining and Metallurgical Engineering*, Vol. 42, No. 3, pp. 14–17, 2022.
- [9] Y. Wei, F. Wang, and Q. Ren, “Numerical simulation of surface subsidence caused by underground mining using discrete element software PFC2D,” *Mining and Metallurgical Engineering*, Vol. 43, No. 2, pp. 30–34, 2023.
- [10] C. Liu, A. Jiang, and Y. Dong, “Mechanism analysis and numerical simulation for landslide of mountain slope with underground complex goaf,” *Mining and Metallurgical Engineering*, Vol. 42, No. 4, pp. 35–42, 2022.
- [11] Qi Wenbin, Liu Huilin, and Wang Feifei, “Numerical simulation of landslide development process caused by underground mining,” *Mining and Metallurgical Engineering*, Vol. 41, No. 4, pp. 29–37, 2021.
- [12] X. Li et al., “Experimental study on instability mechanism and critical intensity of rainfall of high-steep rock slopes under unsaturated conditions,” *International Journal of Mining Science and Technology*, Vol. 33, No. 10, pp. 1243–1260, Oct. 2023, <https://doi.org/10.1016/j.ijmst.2023.07.009>
- [13] Q. Li, Y. Wang, X. Li, S. Tang, B. Gong, and S. Jiang, “Evolutionary characteristics of the fracture network in rock slopes under the combined influence of rainfall and excavation,” *Bulletin of*

*Engineering Geology and the Environment*, Vol. 84, No. 1, Jan. 2025, <https://doi.org/10.1007/s10064-025-04084-7>

- [14] X. Li, Q. Li, Y. Wang, W. Liu, D. Hou, and C. Zhu, "Effect of slope angle on fractured rock masses under combined influence of variable rainfall infiltration and excavation unloading," *Journal of Rock Mechanics and Geotechnical Engineering*, Vol. 16, No. 10, pp. 4154–4176, Oct. 2024, <https://doi.org/10.1016/j.jrmge.2024.08.019>
- [15] Q. Li, D. Song, C. Yuan, and W. Nie, "An image recognition method for the deformation area of open-pit rock slopes under variable rainfall," *Measurement*, Vol. 188, p. 110544, Jan. 2022, <https://doi.org/10.1016/j.measurement.2021.110544>
- [16] E. Hoek and E. Brown, "The Hoek-Brown failure criterion and GSI-2018 edition," *Journal of Rock Mechanics and Geotechnical Engineering*, Vol. 11, No. 3, pp. 445–463, 2019.
- [17] "Code for investigation of geotechnical engineering," GB50021-2001, China Architecture and Building Press, Beijing, 2009.
- [18] "Code for design of nonferrous metal mining," GB50771-2012, China Planning Press, Beijing, 2012.
- [19] S. Lin et al., "Multi-scale quantitative analysis of grotto sandstone degradation considering inorganic salt phase transitions," *International Journal of Rock Mechanics and Mining Sciences*, Vol. 195, p. 106284, Nov. 2025, <https://doi.org/10.1016/j.ijrmms.2025.106284>
- [20] S. Wang et al., "Microstructural deterioration mechanism and failure mode of water-immersed sandstone under uniaxial compression in Dazu rock carvings," *Engineering Fracture Mechanics*, Vol. 321, p. 111110, May 2025, <https://doi.org/10.1016/j.engfracmech.2025.111110>
- [21] X. Zhou, D. Lu, X. Du, G. Wang, and F. Meng, "A 3D non-orthogonal plastic damage model for concrete," *Computer Methods in Applied Mechanics and Engineering*, Vol. 360, p. 112716, Mar. 2020, <https://doi.org/10.1016/j.cma.2019.112716>
- [22] F. Wang, Q. Ren, and X. Jiang, "Engineering geology and subsidence mechanism of a mountain surface in the Daliang Lead-zinc Ore Mine in China," *Bulletin of Engineering Geology and the Environment*, Vol. 81, No. 11, 2022.
- [23] F. Wang, X. Jiang, and J. Niu, "The large-scale shaking table model test of the shallow-bias tunnel with a small clear distance," *Geotechnical and Geological Engineering*, Vol. 35, No. 3, pp. 1093–1110, Jan. 2017, <https://doi.org/10.1007/s10706-017-0166-3>
- [24] F. Wang et al., "Acceleration and displacement dynamic response laws of a shallow-buried bifurcated tunnel," *Journal of Vibroengineering*, Vol. 21, No. 4, pp. 1015–1029, Jun. 2019, <https://doi.org/10.21595/jve.2019.20445>
- [25] Y. Li, F. Wang, and A. Jiang, "Deformation and failure characteristics and stability of open-pit slopes with fault structure," *Mining and Metallurgical Engineering*, Vol. 44, No. 4, pp. 150–154, 2024.
- [26] "Technical code for non-coal open-pit mine slope engineering," GB51016-2014, China Planning Press, China, 2014.
- [27] C. Ma, D.-C. Lu, X.-L. Du, C.-Z. Qi, and X.-Y. Zhang, "Structural components functionalities and failure mechanism of rectangular underground structures during earthquakes," *Soil Dynamics and Earthquake Engineering*, Vol. 119, pp. 265–280, Apr. 2019, <https://doi.org/10.1016/j.soildyn.2019.01.017>



**Anmin Jiang** obtained a master's degree from Central South University of Forestry and Technology in Changsha, China, in 2015. He is currently a full-time teacher in the Department of Management Engineering at Hunan Urban Construction College.



**Daobing Zhang** received Ph.D. degree in Central South University, Changsha, China, in 2023. He is currently mainly engaged in research in the field of underground engineering.



**Feifei Wang** received Ph.D. degree in Chongqing Jiaotong University, Chongqing, China, in 2023. His current research interests include slope engineering and rock mechanics.



**Yanchen Dong** obtained a master's degree from Central South University of Forestry and Technology in Changsha, China, in 2017. She is currently a full-time teacher in the Department of Management Engineering at Hunan Urban Construction College.



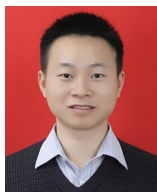
**Huadong Yin** obtained a master's degree from Hunan University of Science and Technology in Xiangtan, China, in 2021. He is currently a doctoral candidate in mining engineering at Hunan University of Science and Technology.



**Huzhi Wang** obtained a bachelor's degree from Beijing Jiaotong University in Beijing, China, in 2011. He is currently the project manager and senior engineer of the First Engineering Co. Ltd. of China Railway Wuju Group.



**Sheng Zhang** obtained a bachelor's degree from Hunan University of Science and Technology in Xiangtan, China, in 2013. He is currently the chief engineer of the project department and senior engineer of the First Engineering Co. Ltd. of China Railway Wuju Group.



**Zhicheng Duan** obtained a master's degree from University of South China in Hengyang, China, in 2013. He is currently an employee of Zhejiang University of Technology Engineering Design Group Co., Ltd.



**Shaoxiang Xie** is currently a Master candidate in mining engineering at Hunan University of Science and Technology.